Interference of Multimode Photon Echoes Generated in Spatially Separated Solid-State Atomic Ensembles

M. U. Staudt,[1] M. Afzelius,[1] H. de Riedmatten,[1] S. R. Hastings-Simon,[1] C. Simon,[1] R. Ricken,[2] H. Suche,[2] W. Sohler,[2] and N. Gisin[1]

[1]*Group of Applied Physics, University of Geneva, CH-Geneva, Switzerland*
[2]*Angewandte Physik, University of Paderborn, 33095 Paderborn, Germany*

(Received 12 July 2007; published 25 October 2007)

High-visibility interference of photon echoes generated in spatially separated solid-state atomic ensembles is demonstrated. The solid-state ensembles were $LiNbO_3$ waveguides doped with erbium ions absorbing at 1.53 μm. Bright coherent states of light in several temporal modes (up to 3) are stored and retrieved from the optical memories using two-pulse photon echoes. The stored and retrieved optical pulses, when combined at a beam splitter, show almost perfect interference, which demonstrates both phase preserving storage and indistinguishability of photon echoes from separate optical memories. By measuring interference fringes for different storage times, we also show explicitly that the visibility is not limited by atomic decoherence. These results are relevant for novel quantum-repeater architectures with photon-echo based multimode quantum memories.

DOI: 10.1103/PhysRevLett.99.173602 PACS numbers: 42.50.Md, 03.65.Yz, 03.67.−a, 42.25.Hz

Broad efforts are currently under way to extend quantum communication to very long distances [1–10]. Existing quantum communication systems are limited in distance mainly due to exponential transmission losses. One approach to overcome this limitation is the implementation of quantum repeaters [1], which have quantum memories [6–8] as the core element. Many proposed quantum-repeater protocols, see, e.g., [3–5], exhibit as a common feature the distribution of entanglement by interference of quantum states of light stored and released from spatially distant quantum memories (QMs). The storage must be phase preserving, as entanglement between remote QMs could not be created otherwise. To obtain reasonable counting rates in quantum communication systems for distances over 1000 km, some form of multiplexing is likely to be required [4,5]. For instance the protocol of Ref. [5] predicts a speed up in the entanglement generation rate by taking advantage of the storage of multiple distinguishable temporal modes (multimodes) in a single quantum memory. Techniques based on photon echoes [11,12] seem well adapted for the storage of multimodes, as photons absorbed at different times are emitted at different times. Multimode storage of classical pulses has been successfully implemented in swept-carrier photon-echo experiments, where up to 1760 modes have been stored and retrieved [13]. The storage of single photons with high efficiency using a photon-echo type scheme is in principle possible with a technique based on Controlled Reversible Inhomogeneous Broadening (CRIB) [14–16], where inhomogeneous rephasing is triggered by an external electric field instead of a strong optical pulse.

Atomic ensembles in the solid state using rare-earth-ion-doped materials seem promising for the implementation of a quantum memory, owing to the absence of atomic diffusion and the long coherence times that are possible for optical and hyperfine transitions [17,18]. For the realization of multimode QMs using photon-echo techniques, long optical coherence times are essential in order to achieve sufficient storage times and high efficiency storage for several temporal modes [5]. Moreover, there is a wide range of wavelengths available using different rare-earth ions. In particular, the Erbium ion has a transition around 1530 nm, where the transmission loss in optical fibers is minimal. First steps towards photonic quantum storage in rare-earth-ion doped materials have been demonstrated using Electromagnetically Induced Transparency [18] and photon echoes approaches [16,19]. Several experiments have shown phase preserving storage of bright pulses in a single optical memory with photon-echo techniques [19–21].

In this Letter, we address the issue of phase preservation in the storage and retrieval of bright coherent states in multiple temporal modes in two different solid-state optical memories, based on the photon-echo technique. The atomic ensembles, separated by 7 cm, are implemented with Erbium ions doped into a $LiNbO_3$ waveguide (WG). We also study the influence of atomic decoherence on phase preservation by varying the storage time. The implementation of CRIB requires an efficient three-level lambda system, which has not been demonstrated in Erbium so far. However, the phase preservation for a CRIB-based quantum memory can be investigated in two-pulse photon-echo-based memory using bright pulses, as phase properties of the storage material will not change.

To investigate the phase preservation, we use first order interference of photon echoes generated in two Erbium-doped $LiNbO_3$ WGs placed in the arms of a balanced Mach-Zehnder interferometer (see Fig. 1). Two-pulse photon echoes are generated in the two ensembles by coherent excitation using two bright pulses, and the photon echoes

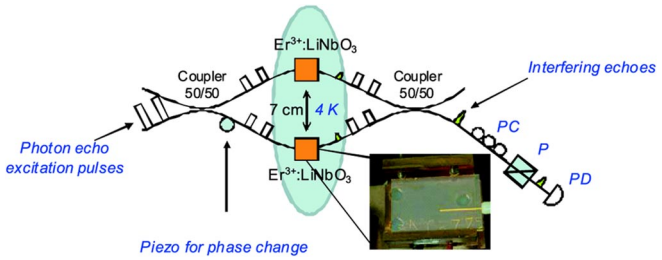

FIG. 1 (color online). Experimental setup: two Er^{3+} : $LiNbO_3$ WGs (a photo of one is shown in the inset) are placed in the arms of a fiber-optic interferometer in a region where the interferometer is at 4 K. While both arms have the same length (2.63 m), in one arm, the fiber is coiled partially around a piezoelectric element, allowing for controlled phase shifts. The excitation light pulses are sent through the interferometer. The generated echoes interfere at the second coupler. In order to project the polarizations onto one axis, we used a polarization controller (PC), a polarizer (P), and a photo detector (PD).

created in each arm interfere at the second beam splitter. The interference fringe visibility is used as a measure of the phase coherence of the memories.

In a two-pulse photon-echo experiment using an inhomogeneously broadened two-level atomic system, a first pulse of area Θ (called data pulse) brings the atoms into a coherent superposition of ground and excited state. A macroscopic dipole moment is produced and decays due to inhomogeneous dephasing. A second pulse, ideally a π pulse (called read pulse) at time t_{12} after the data pulse, will lead to rephasing, and after a time $2t_{12}$, a macroscopic dipole moment is established producing a photon echo. The two-pulse photon echo can be seen as a storage and retrieval of the data pulse, which can also be a sequence of pulses. The time $t_s = 2t_{12}$ is the storage time.

The memories used were two Erbium-doped $LiNbO_3$ crystals with single-mode Ti-indiffused optical WGs (for more details see Refs. [19,22]). The atoms were excited on the $4I_{15/2} \rightarrow {}^4I_{13/2}$ transition at a wavelength of 1532 nm. This transition is inhomogeneously broadened to 250 GHz due to slightly different local environments seen by each Erbium ion [17]. The WGs had a length of about 20 mm, where 10 mm were doped. WG II had 2 times higher Erbium doping concentration than WG I (WG I: $4 \times 10^{19}/\mathrm{cm}^3$ surface concentration before indiffusion), resulting in a higher absorption in WG II. The optical coherence time is limited by magnetic spin interactions between Erbium ions, but can be considerably increased by applying an external magnetic field [23]. A constant magnetic field of about 0.2 Tesla was applied over WG I, and a variable field using a supra-conducting magnet was applied over WG II, both fields being parallel to the C_3 axis of the $LiNbO_3$ crystal. The different magnetic fields and Erbium-doping concentrations resulted in different optical coherence times. The different magnetic fields and Erbium doping concentrations resulted in different optical coherence times, $T_2 = 18$ μs in WG I and $T_2 = 6$ μs in WG II (at around 0.5 Tesla) at a temperature of about 3 K.

The fiber-optic interferometer was placed within a pulse-tube cooler (Vericold). Both arms were installed across a temperature gradient of 300 K, as the couplers had to be placed at ambient temperature. One Er^{3+}-doped $LiNbO_3$ WG was mounted in each arm on the 4 K plate, separated spatially by 7 cm. The photon-echo excitation light pulses had durations of $t_{\mathrm{pulse}} = 15$ ns, and the pulse sequence was repeated at a frequency of 13.5 Hz. This frequency was found to minimize the phase noise of the interferometer due to vibrations in the pulse-tube cooler. The light pulses were created by gating an external-cavity cw diode laser (Nettest Tunics Plus) with an intensity modulator, before amplification by an EDFA (Erbium-Doped Fiber Amplifier). An additional acousto-optical modulator (AA opto-electronics) between the optical amplifier and the input of the pulse-tube cooler, which opened only for the series of pulses, helped to suppress light for all other times even further, thus avoiding spectral hole burning by the EDFA. The input peak powers were in the order of 60 mW (300 mW) for the data (read) pulses, and the released echoes were in the order of a few μW due to the efficiency of the echo process (about 1%) and losses in the interferometer.

In order to obtain high-visibility interference fringes with the retrieved photon echoes, two criteria must be fulfilled. (1) The storage must be phase preserving (i.e., the two echoes must have a fixed phase relation), and (2) the photon echoes must be indistinguishable in order to avoid which-path information. In order to satisfy the second criterion, the echoes from the two ensembles must be detected in the same spatial, polarization and spectral or temporal mode. Moreover, the intensities of the two echoes in front of the detector must be the same. Spatial indistinguishability is ensured by the fact that the interferometer is completely single mode, owing to the use of single-mode fibers and WGs. The polarization of the photon echoes could in principle be adjusted by using polarization maintaining fibers or by inserting polarization controllers inside the interferometer. For technical reasons, we chose instead to project the two photon echoes on a common polarization axis, by inserting a polarizer and a polarization controller before the photo detector (see Fig. 1). Since the generation of photon echoes is a nonlinear process, the spectral/temporal modes of the echoes depend strongly on the intensity of the excitation pulses and on the optical depth [24]. Since the two WGs have different absorption depths, the temporal shape could therefore be adjusted by tuning the wavelength of the excitation laser within the absorption profile. Finally, to equalize the intensity of the echoes, we used an ultrahigh precision translation stage system (anp, attocube systems) to change the in and out coupling powers. Moreover, by adjusting the magnetic field for WG II, one can change the optical coherence time, and thus change the amplitude of the photon echo.

In order to characterize the phase noise of the interferometer, we measured interference fringes using a cw-off-

resonant laser at $\lambda = 1550$ nm. While scanning the phase as the pulse-tube was cooling, a visibility close to 92% was obtained, limited by phase noise introduced by the vibrations of the cooling system. By shutting down the cooling system for a short time, we obtained a visibility close to 100%. Thus for all photon-echo measurements, which had to be carried out below 4 K, a visibility of 92% was an upper technical limit.

We first discuss the experiments carried out on the storage of a single temporal mode. In these experiments, the storage time was fixed at 1.6 μs. Figure 2(a) shows interfering photon echoes for constructive and destructive interference. By scanning the phase difference of the interferometer continuously, interference fringes were obtained. An example is shown in Fig. 2(b). A visibility of 90.5% ($\pm$ 1.8%) was obtained by averaging over many measurements, which is within the limit set by the intrinsic phase noise due to the cooling system. Therefore, we can conclude that the storage of the optical pulses in the solid-state ensembles is fully phase preserving within the error bars. Moreover, the two paths of the interferometer cannot be distinguished in any of the spatial, polarization, or spectral/temporal modes. Note that high visibilities were achieved even though the WGs had different physical properties, particularly in their absorption coefficients and optical coherence times.

We now turn to the investigation of the storage of multiple modes. The data then contain several pulses separated by 150 ns which coherently excite the atoms. If the intensity of the pulses is well below saturation, each pulse independently generates an echo triggered by the strong read pulse. In Fig. 3, we show examples of interfering photon-echo signals for two and three modes, both for destructive and constructive interference. The visibility is measured for each mode separately from interference fringes [as in Fig. 2(b)] and is an average over several independent measurements. The average visibility is only slightly reduced from 90.5% for the case of the storage of one mode to 86.9% for the lowest value out of the three stored modes. Thus, we show that high-visibility storage of multiple modes in independent solid-state optical memories is possible. In the case of only one stored mode, all parameters (intensity, pulse length, coupling, etc.) were optimized in order to obtain a strong photon-echo signal from both WGs. For the case of two and three stored modes, optimization is experimentally more demanding, as one has to work in a regime where each of the data pulse areas Θ has to be much smaller than $\pi/2$. Otherwise, echo distortion and additional undesired multipulse echoes that might interfere with the echoes of the data pulses will occur. Moreover, the issues related to different optical depths in the two crystals mentioned above [24] are even more critical in the case of multiple modes, since optimization of one mode does not guarantee the indistinguishability of the other modes. These issues together with the detector sensitivity were the main limitations for the number of modes that could be stored. Overcoming these technical issues, the enlargement of the storage capacity should be possible. By implementing a CRIB-type scheme, storage of even more modes should be possible [5].

Finally, we study the effect of atomic decoherence on the emitted photon echoes. The optical coherence in solid-state systems is perturbed by interaction with the environment, leading to atomic decoherence. In Erbium-doped $LiNbO_3$, this dephasing arises from interactions between the large Er^{3+} magnetic moment and fluctuating local magnetic fields due to changing magnetic spins on neighboring Er ions, so-called spin flips [17]. The atomic decoherence will cause an exponential decay of the two-pulse photon-echo signal, as exemplified for WG II in Fig. 4. From this decay of the photon-echo signal, a T_2 of 6 μs was measured.

In an optical memory, ideally the phase should be preserved independently of the storage time. At first sight, this might seem to be a contradiction due to the unavoidable atomic decoherence. To test the influence of atomic decoherence on the visibility, we measured interference fringes as a function of the storage time (0.8 μs to 5.6 μs, as shown in Fig. 4). We found that although the photon-echo amplitude decreases strongly due to atomic decoherence in this time period, the visibility is unaffected and remains at

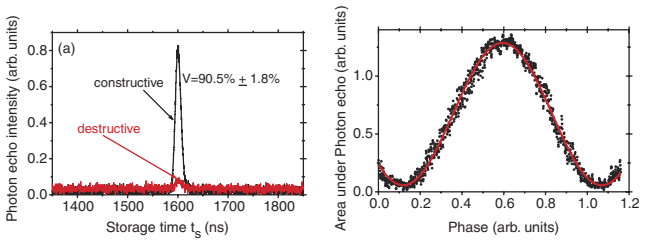

FIG. 2 (color online). (a) Intensity of photon echoes for constructive and destructive interference. (b) Interference fringe: The area under the interfering photon echoes generated in two spatially separated WGs is shown as a function of phase difference. The storage time was set to 1.6 μs. Each point is averaged over 10 echoes, and the measurement of a whole fringe takes about 10 minutes. For this particular fringe, a visibility of $V = 91.5\%$ is reached (averaging over many measurements gives a visibility of 90.5%), limited by phase noise caused by vibrations in the cooling system.

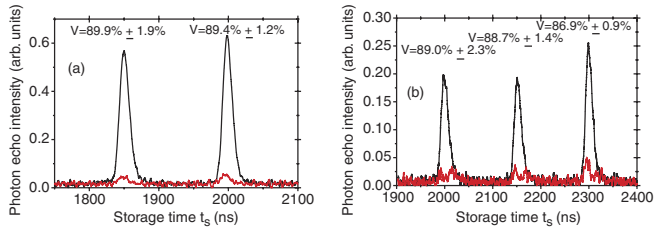

FIG. 3 (color online). Multimode storage: Constructive and destructive photon-echo interference is shown for a storage time of 2 μs for two and 2.3 μs for three stored modes (values for the longest stored mode). Phase coherence is in the two cases preserved to a very high degree as indicated by high fringe visibilities.

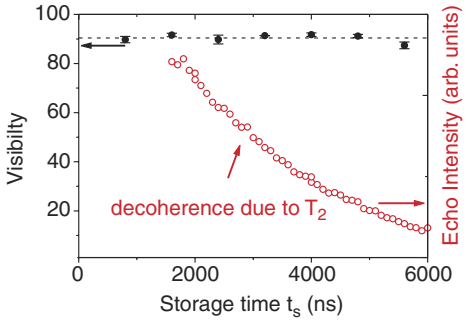

FIG. 4 (color online). Interference fringe visibility (filled circles) is shown as a function of the memory storage time. Atomic decoherence strongly acts on the amplitude of the echo signal, as shown here for WG II (open circles), but leaves the visibility unaffected. The dotted line shows the average visibility of 90.5%. For each storage time, we readjusted all experimental parameters, as the optical coherence times are different in the two WGs.

90.5%. This can be interpreted as follows: the photon-echo signal is a coherent collective signal, which is due to interference of the photon emission amplitudes from the whole atomic ensemble [25,26]. Its intensity is proportional to $(N\text{-}N')^2$, where N is the total number of atoms and N' is the number of decohered atoms. Atoms having lost their coherence due to interaction with the environment do not contribute to the collective photon-echo emission. Besides the collective coherent emission in the forward mode, there is also an incoherent emission from all atoms, which would be there even without a data pulse, and whose total intensity in the forward spatial mode scales only with N. Therefore, the ratio of the collective photon-echo emission to the incoherent background emission is $(N\text{-}N')^2/N$. Since N is a very large number ($N \sim 10^8$), we detect only the coherent collective part of the signal, even if N' is comparable to N. Thus, it is within expectation that the decay in photon-echo amplitude has no effect on visibility. This holds as long as the background noise from other sources than the photon-echo process itself is much smaller than the photon-echo amplitude, as is the case in this experiment. Note in this context that CRIB is also a collective process. Thus the atomic decoherence should not influence the phase preservation for a CRIB-type memory either.

Note that in the context of quantum communication, only the photons reemitted from the memories and detected contribute to the signal. Hence, in our case, atomic decoherence, which acts only as a loss, will affect the efficiency of a given protocol, but not the effective fidelity. In that sense, the visibility of the interference fringe can be considered as a measure of the effective fidelity of the storage and retrieval in the memory.

In conclusion, we show that phase coherence is preserved to a high degree in the storage and retrieval of light pulses in spatially separated solid-state atomic ensembles using photon-echo techniques. This phase coherence is revealed in interference patterns that show a visibility of 90.5% ($\pm$1.8%), close to the technical limit of 92% set by phase noise caused by the cooling system. Extending our studies to three stored temporal modes only leads to a slight decrease in visibility, mainly due to the nonlinear character of the photon-echo storage process. Atomic decoherence due to interactions with the environment does not affect the visibility; i.e., it causes only a loss of signal amplitude, but not a loss of phase coherence of the reemitted optical pulses. This is explained by the collective character of the photon-echo process. These results are interesting in the framework of proposed novel quantum-repeater architectures, where storage and retrieval with high phase coherence preservation and in multiple modes is highly advantageous.

We would like to thank G. Fernandez, M. Legré, and C. Barreiro for assistance and W. Tittel for discussions. We are grateful for support by the Swiss NCCR Quantum Photonics and by the EU Integrated Project Qubit Applications.

[1] H. J. Briegel *et al.*, Phys. Rev. Lett. **81**, 5932 (1998).
[2] N. Gisin and R. Thew, Nat. Photon. **1**, 165 (2007).
[3] L.-M. Duan *et al.*, Nature (London) **414**, 413 (2001).
[4] O. A. Collins *et al.*, Phys. Rev. Lett. **98**, 060502 (2007).
[5] C. Simon *et al.*, Phys. Rev. Lett. **98**, 190503 (2007).
[6] T. Chanelière *et al.*, Nature (London) **438**, 833 (2005).
[7] M. D. Eisaman *et al.*, Nature (London) **438**, 837 (2005).
[8] C. W. Chou *et al.*, Science **316**, 1316 (2007).
[9] A. D. Boozer *et al.*, Phys. Rev. Lett. **98**, 193601 (2007).
[10] P. Maunz *et al.*, Nature Phys. **3**, 538 (2007).
[11] N. A. Kurnit *et al.*, Phys. Rev. Lett. **13**, 567 (1964).
[12] T. W. Mossberg, Opt. Lett. **7**, 77 (1982).
[13] H. Lin *et al.*, Opt. Lett. **20**, 1658 (1995).
[14] S. A. Moiseev and S. Kröll, Phys. Rev. Lett. **87**, 173601 (2001).
[15] M. Nilsson and S. Kröll, Opt. Commun. **247**, 393 (2005).
[16] A. L. Alexander *et al.*, Phys. Rev. Lett. **96**, 043602 (2006); G. Hétet *et al.*, arXiv:quant-ph/0612169.
[17] Y. Sun *et al.*, J. Lumin. **98**, 281 (2002).
[18] J. J. Longdell *et al.*, Phys. Rev. Lett. **95**, 063601 (2005).
[19] M. U. Staudt *et al.*, Phys. Rev. Lett. **98**, 113601 (2007).
[20] M. Arend *et al.*, Opt. Lett. **18**, 1789 (1993).
[21] A. L. Alexander *et al.*, J. Lumin. **127**, 94 (2007).
[22] I. Baumann *et al.*, Appl. Phys. A: Mater. Sci. Process. **64**, 33 (1997).
[23] T. Böttger *et al.*, Phys. Rev. B **73**, 075101 (2006).
[24] T. Wang *et al.*, Phys. Rev. A **60**, R757 (1999).
[25] I. D. Abella *et al.*, Phys. Rev. **141**, 391 (1966).
[26] R. H. Dicke, Phys. Rev. **93**, 99 (1954).